Computer Assisted Mechanics and Engineering Sciences, 4: 127–155, 1997.

Finite element solutions with Walsh series and wavelets

J.A. Teixeira de Freitas and L.M.S. Santos Castro
Departamento de Engenharia Civil, Instituto Superior Técnico
Av. Rovisco Pais, 1096 Lisboa Codex, Portugal

(Received May 27, 1996)

Walsh series and wavelets are nowadays widely applied in digital processes. Their use as approximation functions in a hybrid-mixed finite element formulation for elastic-plastic structural analysis is presented. This formulation is based on the direct approximation of the stress, displacement and plastic multiplier fields in the domain of the finite elements. The displacements on the boundary of the elements are also approximated independently. The essential characteristics and properties of the Walsh and wavelet approximation functions are reviewed. The performances achieved in the different solution phases of elastic and elastoplastic problems are illustrated with numerical applications.

1. Introduction

Typical of the hybrid-mixed finite element formulations is the feature that none of the fundamental relations governing the response of the structure is required to be locally satisfied [1]. This feature allows for the use of virtually any function in setting up the approximation bases and suggests immediately the selection of *computer-friendly* functions in the implementation of the hybrid-mixed formulations.

A computer-friendly approximation basis should be hierarchical, orthogonal and easy to process in a digital environment. The hierarchical nature of the approximation basis is important to support p-adaptive processes and, in particular, the development of *superelements* in order to implement the formulation on a coarse mesh of few but very rich elements. Pre-processing is thus greatly simplified because the dependency on efficient mesh processing tools is minimised and the possibility of using parallel processing is enhanced. Orthogonality is also an important feature, as it provides for highly sparse systems, thus contributing to the reduction of the storage requirements and to the stabilisation of the system solution procedures. Easiness in the numerical processing of the approximation functions is essential in every phase of the calculations but it can be exploited to the point of avoiding completely all the operations of numerical integration and, in some cases, differentiation.

To this effect, three different types of hierarchical orthogonal bases have been tested. The first two use conventional functions, namely trigonometric functions and Legendre polynomials [2, 3]. Considering the importance of the role played by digital computers in the implementation of the finite element method, the hybrid-mixed formulations were also selected [4] to host the testing of Walsh series and wavelets, the special functions used presently to support many applications in digital environments. Due to their natural ability to blend in such environment, the Walsh series [5] and the wavelets [6] are nowadays essential to developments in such distinct fields as spectroscopy, seismology, speech processing and data compression [7–11]. In particular, it was the successful use of Walsh series and wavelets in image processing that first motivated its application in the finite element modelling of structural analysis problems [12].

The objective of the paper is to present an overall view of the implementation of hybrid-mixed finite elements using digital interpolation functions. In the first part of the paper the basic rea-

sons that led to the involvement in the research on hybrid-mixed finite element formulations are briefly enumerated and the results achieved with its combination with Walsh series and wavelets are qualitatively assessed. Next, the essential properties of these functions are stated and their manipulation in the context of the implementation of finite element models is described. The third part of the paper is dedicated to the presentation of the finite element formulation being used. It is derived from the fundamental structural relations involved and the associated energy statements are obtained using mathematical programming [13, 14]. The important role that mathematical programming can play in the field of structural analysis, in both the theoretical and the numerical aspects, is recalled. The last part of the paper focuses on computational aspects. The use of Walsh series and wavelets to support the finite element model is analysed in the different phases of the calculations and illustrated with numerical applications.

2. Motivation

The dominant trend in the developments taking place in the field of computational structural mechanics is to model and solve efficiently increasingly more realistic and complex problems using a well established and proven tool, the displacement formulation of the finite element method. The extent of the success of the conforming element is so overwhelming that fellow researchers often question the worthiness of studying alternative finite element formulations.

Among the different reasons one might enumerate to justify this study, the following two seem to be of particular relevance in the present context. Firstly, one is led to question the basic concepts from which the design of a tool has evolved when a substantial investment is being dedicated either to overcome limitations intrinsic to essential aspects of the design of the tool or to develop supporting tools for the same effect. This is the case with the conforming element in some aspects.

For instance, meshing became an autonomous discipline and the implementation of meshing procedures may consume means that cannot be neglected in relation to those corresponding to the implementation of the finite element solver it is designed to support. Secondly, the dependence of the finite element method on the computer hardware is so strong that one must question if it is being written in the most friendly format for digital environments and whether the encodement of the method is the best suited to exploit the current developments in computer technology, namely in what concerns parallel processing.

Looking back onto the development of the information technology from a computational structures stand point, three features seem to characterise the replies found for the questions stated above; enhancement of parallel processes, relaxation of local conformity constraints in favour of averaged and hierarchical information, and the use of binary supports in detriment of continuous supports.

A problem common to most areas directly supported by information technology is to create efficient processes to generate images of complex systems at high speed and with variable levels of requirements in terms of on accuracy. That is also the central problem in computational structures, the *image processing* of the stress, strain and displacement fields. To import the image processing techniques into the finite element method means, presently, to approximate the structural fields using digital functions, instead of polynomials and other C-class functions, in support of a formulation released from strong constraints on the local solution of field equations and boundary conditions. It seems that this degree of flexibility is best exploited through the hybrid-mixed formulations of the finite element method.

3. Basic features

Geometrically linear, quasi-static, elastic and elastoplastic problems are used here to illustrate the use of Walsh series and wavelets in hybrid-mixed finite element solutions. The essential features of the finite element formulation and of the numerical advantages that can be secured by using these special approximation functions are stated next.

3.1. Finite element formulation

In the hybrid-mixed formulation for elastic-plastic elements used here, four fields are approximated independently. These are, in the domain of the element, the stresses, the displacements and the plastic multipliers. The displacements are simultaneously approximated on the boundary of the element. The kinematic boundary conditions and the plastic flow conditions are enforced locally. The remaining field equations and boundary conditions, namely equilibrium, compatibility, elasticity, the yield rule and the static boundary conditions are enforced in weighed residual form.

The approximation criteria are so defined as to ensure that the finite element model embodies the fundamental properties that typify the structural problem under analysis, namely, *static-kinematic duality* (the equilibrium and compatibility operators are adjoint) elastic reciprocity (the elasticity matrix is symmetric) and *associated plasticity* (the plastic multiplier rates are orthogonal to the yield surface). Consequent upon the preservation of these fundamental properties, the non-linear system of equations and inequalities relating to the elastic-plastic behaviour of the structure is encoded as a symmetric complementarity problem.

Finite element formulations are usually derived from energy statements, which sometimes are adapted to accommodate the approximation criteria that are to be enforced. To control directly the approximations and to better expose their physical meaning, the finite element formulation is here derived from the fundamental relations governing the structural problem under analysis. The associated energy statements are recovered by processing the finite element governing system through mathematical programming equivalence theory, which can also be used to establish conditions for the existence, uniqueness and stability of the solutions [15, 16].

Finite element solving systems have high sparsity indices. This property is enhanced in the hybrid-mixed formulations because element interdependency is even more localised. In the stress model used here, this dependency reduces to the interelement traction continuity conditions, which affect pairs of neighbouring elements. All the remaining conditions are strictly element dependent. This is the property that renders the hybrid-mixed formulations so appealing for parallel processing.

A general asymptotic expansion technique is used to replace the governing complementarity problem by an equivalent sequence of recursive linear systems, which is solved using a variant of the Simplex algorithm [17]. The incremental process of analysis is based on the implementation of simple rules to determine automatically the step length that exposes the activation or deactivation of plastic yield modes, or the mobilisation of collapse mechanisms. The operation of this algorithm is coupled with the available procedures to store and solve efficiently large sparse systems [18, 19].

Substantial gains can also be achieved in the post-processing phase. The graphic representation of the relevant structural fields is simplified because the stresses, the displacements and the increments on the plastic multipliers are directly approximated.

3.2. Approximation functions

It is the fact that none of the field equations and boundary conditions have to be satisfied locally that opens up the possibility of supporting the implementation of hybrid-mixed formulations by a wide range of approximation functions, in replacement of the polynomials traditionally used in finite element codes. Of the many alternatives possible, the Walsh series and the wavelets seem to be the ones that are best positioned to exploit the digital environment in which the computers operate.

The basic operations involved in the finite element calculations, namely sums, products, derivatives and integrals, can be processed at high speed by using binary algorithms. Moreover, the simplicity of the functions is such that in most cases it is possible to derive general analytical expressions for the coefficients of the finite element matrices, thus avoiding completely the implementation of numerical integration and differentiation procedures [20–22].

These functions enjoy two other important properties; they are *hierarchical* and *orthogonal*. The hierarchical nature of the approximation functions enhances the use of coarse meshes of very rich

elements and simplifies the direct implementation of adaptive procedures. As a consequence of the strong orthogonality properties they enjoy, the finite element matrices generated through these functions have very high sparsity indices, which allows for substantial gains in storage requirements.

In the post-processing phase the speed in the computation of the graphic outputs is high not only because these functions are so simple to operate but also because efficient transformation techniques, similar to the fast Fourier transforms, can be implemented to support the representation of the static and kinematic fields characterising the response of the structure.

4. LIMITATIONS

Four aspects should be stressed in identifying the limitations detected in the implementation of hybrid-mixed formulations based on Walsh series and wavelets. Two of them relate directly with the approximation functions: the dimension of the solving systems generated through Walsh series and the level of expertise required by the handling of these series and wavelets. The hybrid-mixed finite element formulation itself is responsible for the other two limitations: the formulation is not particularly easy to understand and control by everyday users and is susceptible to the emergence of spurious modes.

4.1. Approximation functions

The Walsh series is based on very rudimentary functions that can take only two values, $+1$ and -1. Consequently, the crispness of the images of continuous fields produced with Walsh functions is strongly dependent on the number of terms taken in the series approximation. Therefore, high accuracy levels in the finite element representation of structural responses modelled with Walsh series lead, in general, to solving systems with very large dimensions. However, they are still a very competitive tool because of the levels of efficiency they provide in terms of processing speed and storage requirements in the phases of pre-processing, solving and post-processing of the finite element model.

Wavelets can be crudely described as higher-order digital functions. They share most of the properties that make the use of the Walsh series so attractive in the computer solution of structural mechanics problems. The wavelets may not be as easier to manipulate as the Walsh series but, because they contain a much richer functional information, they allow for a substantial reduction in the number of degrees of freedom necessary to attain equivalent levels of accuracy in the representation of finite element solutions.

The efficient use of the Walsh series and wavelets is strongly dependent on the appropriate use of highly specialised handling techniques. The use of these functions in the context of computational structures without the support of such techniques is simply unpracticable. Because these functions and the supporting techniques are so alien to the studies in computational mechanics and because the developments in microelectronics are happening at such a high pace, developers of finite elements for computational structures have a very difficult task in ensuring that proper use is being made of the currently available technology. For instance, during the first year of the studies reported here the improved understanding and the progressive incorporation of appropriate techniques allowed the CPU time required to solve the same particular problem to be reduced from a few hours to a few seconds.

4.2. Finite element formulation

Susceptibility to spurious modes is the weakest characteristic of the hybrid formulations and one that is yet to be solved in convenient, practical terms. Spurious modes can affect the conventional, displacement formulation, where, however, they are easier to detect and block at the development

level. The difficulty with hybrid-mixed formulations is that the detection *a priori* of spurious modes is still expensive, for instance through the use of singular value decomposition techniques, and efficient preventive measures are yet to be readily available [23]. However, it is important to challenge the established view that this is a fatal weakness that renders the hybrid-mixed formulations useless. On the contrary, it is indeed a limitation worth to live with to be able to exploit the particular advantages that this type of formulation offers.

The technique suggested in Ref. [24] consists in developing a macro-element as an assemblage of elements so devised as to assign the potential spurious modes to internal variables in order to ensure the positive-definiteness of the solving system. The procedure adopted here is rather more simplistic. Scalar conditions related to the static and kinematic indeterminacy numbers of the elements are stated *a priori* to minimise the possibility of occurrence of spurious modes. At the implementation level, the system solvers are adapted to discard automatically the dependent modes that may persist. In this unlikely but possible situation, the solution that is obtained is still useful, as only one of the displacement fields, in the domain or on the boundary, is affected by the spurious modes. The unaffected displacement approximation is still usable as well the estimate obtained for the stress field.

The second major reason for the relative success of the displacement formulations with respect to the hybrid formulations is that they are easier to understand and to control. Controlling is directly related to the fact that the hybrid-mixed formulations are naturally hierarchical. The user can assign different degrees of approximation to the different fields in the element and from element to element. This degree of flexibility is such that users must spend a relatively higher amount of time and effort to understand and control the consequences of manipulating the different parameters that may be involved in the alternative hybrid-mixed finite element formulations. Therefore, the successful use of such a tool in a commercial environment is highly dependent on the existence of robust, automatic adaptive procedures.

5. WALSH SERIES

The orthogonal basis suggested by Walsh [5] is formed by an ordered set of rectangular waveforms taking only two possible amplitude values, $+1$ and -1. They have compact support, meaning that they are defined over a finite *time/space* interval, and require two parameters for complete definition, a *time* period t and an ordering number n related to *frequency*.

Represented in Fig. 1 are the first eight terms of the complete series that can be built from Walsh functions, $WAL(n,t)$, ordered in ascending value of the number of crossings found within the time basis. This ordering of the functions, originally proposed by Walsh, known as the *sequency ordering*, is the closest to the common practice with orthogonal functions; Fourier series are also arranged in increasing harmonic numbers. It is the ordering used in the present finite element applications. Alternative ordering criteria, more appropriate for particular applications, are suggested in the literature [25, 26].

Generalisation to n dimensions is straightforward. Figure 2 shows the first 64 terms of the two dimensional Walsh sequence. Each function, denoted by $WAL(n,x)WAL(m,y)$, is obtained from the direct product of the corresponding one dimensional Walsh functions.

The following operations involving Walsh functions are relevant in the implementation of computational mechanics problems: generation of the functions, linear combination, multiplication, differentiation and integration. The algorithms used in the manipulation of Walsh functions in the context of finite element solutions can be found in [20]. These algorithms exploit three fundamental properties of the Walsh functions: they form a complete series of orthogonal functions, they are symmetric with respect to the order and time parameters, and are closed under multiplication, meaning that the product of two Walsh functions is still a Walsh function.

Alternative methods have been suggested to generate Walsh functions. The methods discussed in [20] are the generation from recursive relations, the application of Chien's equation, the successive

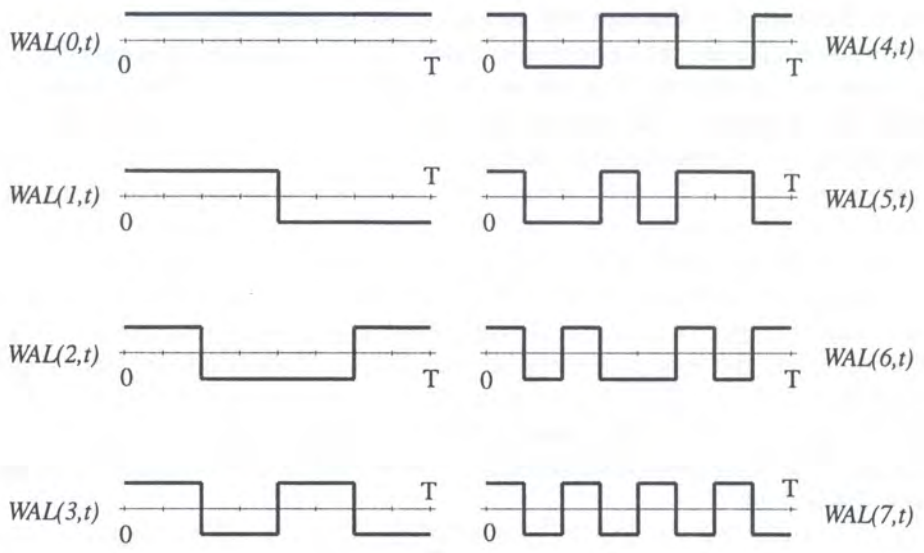

Fig. 1. One-dimensional Walsh functions.

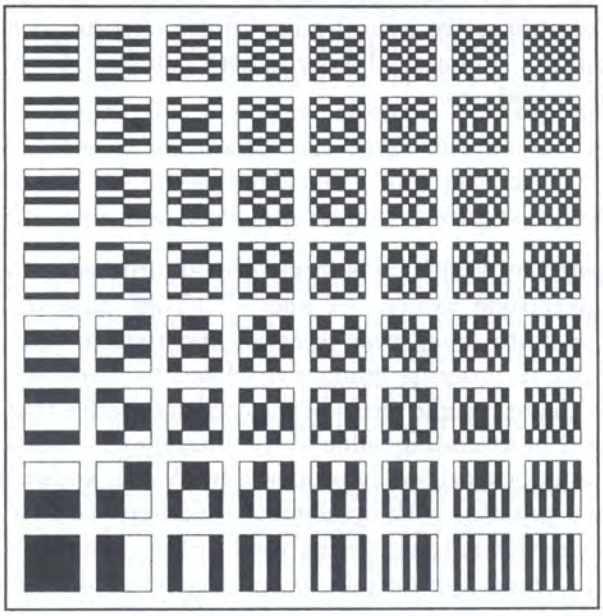

Fig. 2. Two-dimensional Walsh functions.

products of Rademacher functions, and the use of the Hadamard matrix. The recursive methods seem to meet best the specific requirements of finite element applications, which are based on complete series of Walsh functions. Table 1 shows the CPU time spent to compute the information required to define the first $N = 2^p$ Walsh functions using this method. For each function, the amplitude, -1 or $+1$, for each of the N sub-intervals in which the time basis is divided is computed and stored. A workstation IBM risc 6000/550 is used.

Of central importance for the finite element calculations are the discrete and fast Walsh transforms. Similarly to the Fourier series expansion, a function $f(t)$ can be expressed as the weighed

Table 1. CPU time (miliseconds) required to generate Walsh functions.

N	4	8	16	32	64	128
Time	0.017	0.041	0.133	0.488	2.123	10.871

sum of Walsh functions:

$$f(t) = \sum_{n=0}^{\infty} X_n WAL(n,t),$$

$$X_n = \frac{1}{T}\int_0^T f(t)WAL(n,t)\,\mathrm{d}t.$$

The definitions above apply to a continuous function within a time basis interval $0 \leq t \leq T$. It is convenient for numerical use to consider discrete series of N terms set up by sampling the continuous function at N equally spaced points over the definition interval. N is taken as a power of two to ensure the correspondence of the properties of the continuous and discrete systems. Using the trapezium rule, the integration in the equation above is replaced by the summation of N sampling points to yield the following definition for the finite discrete Walsh transform:

$$X_n = \frac{1}{N}\sum_{i=0}^{N-1} x_i WAL(n,i),$$

$$x_i = \sum_{i=0}^{N-1} X_n WAL(n,i).$$

Illustrated in Fig. 3 is the Walsh series approximation of the trigonometric function $\sin(2\pi t)$. Shown in Table 2 are the CPU times required to compute the expansion for the different values of

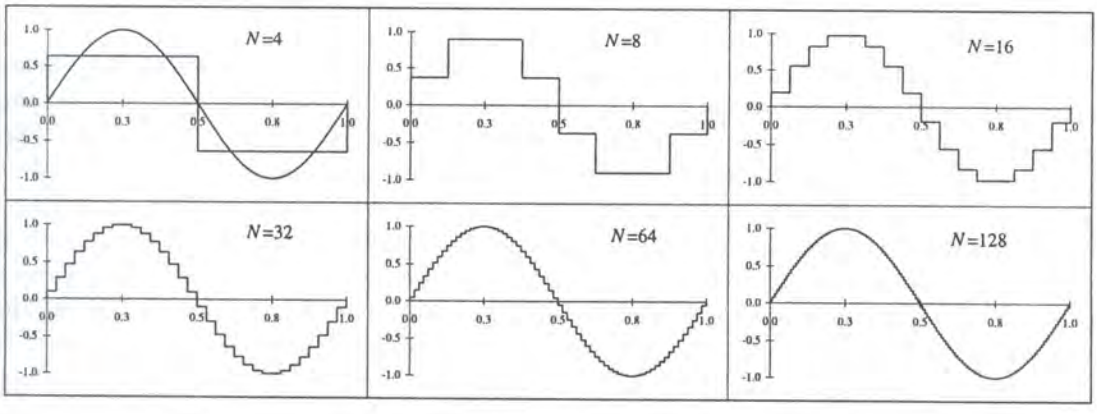

Fig. 3. Walsh approximation of function $\sin(2\pi t)$.

N using 1 and 5 Gauss points, denoted by Time_1 and Time_5, respectively. The improvement in the precision using the latter method is irrelevant for $N > 4$. The direct computation of the Walsh coefficients requires $N(N-1)$ additions and subtractions. However, by using the fast Walsh transform algorithm only $N\log_2 N$ operations are executed. The CPU times required to obtain the coefficients of the expansion illustrated in Fig. 3 using this algorithm are also given in Table 2.

Table 2. CPU time (millisecond) required to compute the Walsh Transform (WT) and the Fast Walsh Transform (FWT).

Type	N	4	8	16	32	64	128
WT	Time_1	0.2	0.3	0.9	3.5	13.7	55
WT	Time_5	0.3	0.7	2.6	10.5	41.9	166
FWT	Time	0.01	0.02	0.03	0.08	0.14	0.28

6. WAVELETS

The families of compactly supported wavelets introduced by Daubechies [6] form complete series of orthonormal functions and lead to an unconditional basis suitable for a wide range of function spaces. What renders wavelets so interesting is the fact that they are very localised both in frequency and in space. A wavelet system has compact support only if a finite number of wavelet coefficients is non-zero. Wavelet systems are partitioned into families according to its wavelet number N, which is usually one-half of the number of non-zero coefficients.

To obtain each one of the Daubechies wavelet families, it is necessary first to derive two functions, the scaling function $\phi(x)$ and the primary wavelet $\psi(x)$. These functions are defined recursively [10] as linear combinations of scaled and shifted versions of $\phi(x)$:

$$\phi(x) = \sum_{k \in Z} c_k \, \phi(2x - k),$$

$$\psi(x) = \sum_{k \in Z} (-1)^k c_{1+k} \, \phi(2x + k).$$

It is from restrictions on the values of the wavelet coefficients, c_k, that the wavelet functions derive their properties, namely orthonormality. The complete Wavelet system is then generated by taking translations and dilations on both the scaling function and the primary wavelet:

$$\phi_{j,k}(x) = 2^{j/2} \, \phi(2^j x - k); \quad j, k \in Z,$$

$$\psi_{j,k}(x) = 2^{j/2} \, \psi(2^j x - k); \quad j, k \in Z.$$

In the case of Daubechies families of functions, $N-1$ is the maximum degree of the polynomials which can be exactly represented by a linear combination of the translates $\phi(x-k)$. Daubechies presents families of functions with the wavelet number ranging from $N = 2$ to $N = 10$. Figure 4 shows the scaling function and primary wavelet for some of these families.

Scaling functions do not have analytical expressions. They have to be generated recursively from the dilation equation. Daubechies obtains and presents the values of the wavelet coefficients for all of the wavelet families studied. The wavelet coefficients can be derived by imposing three basic conditions: the area under the scaling function is set to unity; the scaling function is required to be orthogonal to all its translates; and the primary wavelet is required to be orthogonal to the elementary polynomials x^n, to ensure that polynomials of less or equal to $n = N - 1$ are exactly represented by a linear combination of the scaling function and its integer translates. The wavelet coefficients are thus found to satisfy the following conditions [9]:

$$\sum_{k \in Z} c_k = 2,$$

$$\sum_{k \in Z} c_k \, c_{k+2m} = \delta_{0m}, \qquad m \in Z,$$

$$\sum_{k \in Z} c_k \, (-1)^k \, k^m = 0, \qquad m = 0, 1, \ldots, N-1.$$

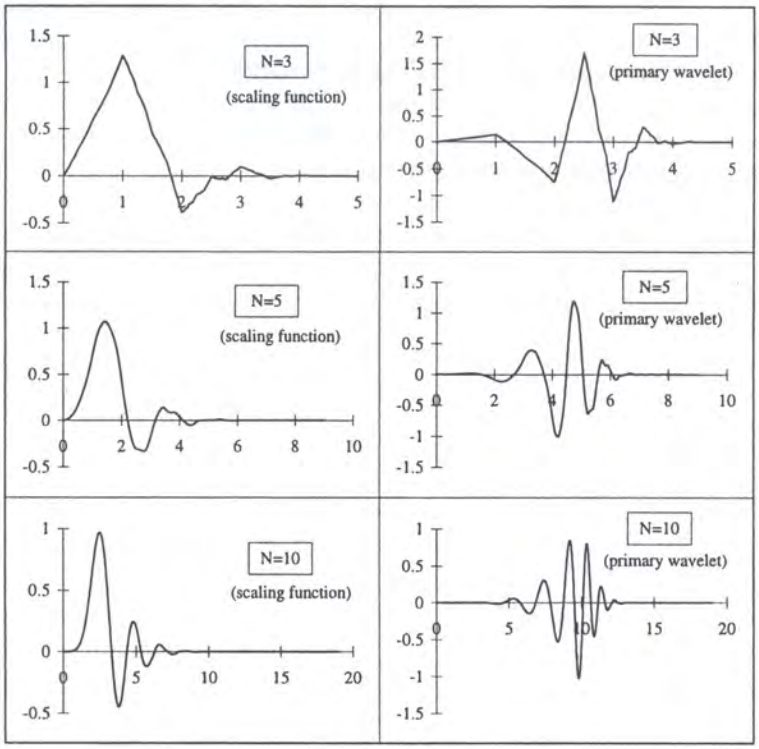

Fig. 4. Scaling functions and primary wavelets.

There are alternative forms to expand functions in a wavelet basis. The results shown in Fig. 5 represent the expansion of the trigonometric function $\sin(2\pi x)$ by applying the expression,

$$f(x) = \sum_{k \in Z} c_{m,k}\, \phi_{m,k}(x)$$

with

$$c_{m,k} = \int \phi_{m,k}(x)\, f(x)\, \mathrm{d}x,$$

and $m = 0$ for every case. Figure 6 illustrates the expansion of the same trigonometric function but taking now different values for m and using wavelets with $N = 3$.

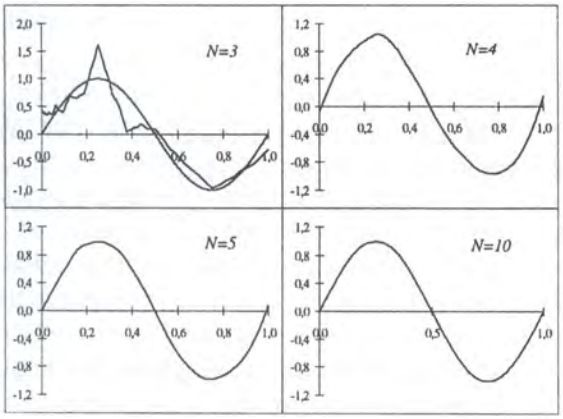

Fig. 5. Approximation with $m = 0$.

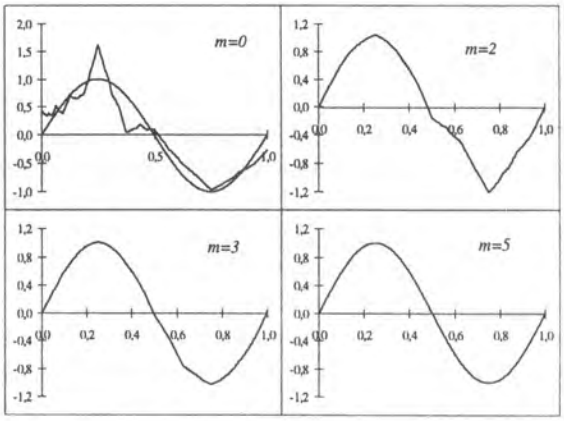

Fig. 6. Approximation with $N = 3$.

Extension of orthogonal wavelet systems into R^n is obtained by the direct product of n one dimensional wavelet functions. The basic operations involved in finite element computations based on wavelet approximation functions are discussed in Ref. [22].

7. FUNDAMENTAL STRUCTURAL RELATIONS

The fundamental relations governing the elastoplastic response of the domain V enclosed within a surface Γ are summarised below; Γ_σ and Γ_u denote complementarity regions of the enveloping surface whereon tractions t_Γ and displacements u_Γ are prescribed, respectively.

$$\mathbf{D}\boldsymbol{\sigma} + \mathbf{b} = \mathbf{0} \quad \text{in } V, \tag{1}$$

$$\boldsymbol{\varepsilon} = \boldsymbol{\varepsilon}_\mathrm{e} + \boldsymbol{\varepsilon}_\mathrm{p} = \mathbf{D}^*\mathbf{u} \quad \text{in } V, \tag{2}$$

$$\mathbf{N}\boldsymbol{\sigma} = \mathbf{t}_\Gamma \quad \text{on } \Gamma_\sigma \tag{3}$$

$$\mathbf{u} = \mathbf{u}_\Gamma \quad \text{on } \Gamma_u \tag{4}$$

$$\boldsymbol{\varepsilon}_\mathrm{e} = \mathbf{f}\boldsymbol{\sigma} + \boldsymbol{\varepsilon}_\theta \quad \text{in V}, \tag{5}$$

$$\Delta\varphi_* = -h\Delta\varepsilon_* + \mathbf{n}^\mathrm{T}\Delta\boldsymbol{\sigma} + R_\varphi, \tag{6}$$

$$\varphi_* + \Delta\varphi_* \leq 0, \tag{7}$$

$$\Delta\boldsymbol{\varepsilon}_\mathrm{p} = \mathbf{n}\Delta\varepsilon_* + \mathbf{R}_\varepsilon, \tag{8}$$

$$\Delta\varepsilon_* \geq 0, \tag{9}$$

$$\varphi_*\Delta\varepsilon_* = 0, \tag{10}$$

$$\Delta\varphi_*\Delta\varepsilon_* = 0. \tag{11}$$

In the equilibrium and compatibility conditions (1) and (2), $\mathbf{b}$ and $\mathbf{u}$ are the displacement and body force and displacement vectors, respectively, and $\boldsymbol{\sigma}$ and $\boldsymbol{\varepsilon}$ represent the vectors where the independent components of the stress and strain tensors are collected, respectively; addends $\boldsymbol{\varepsilon}_\mathrm{e}$ and $\boldsymbol{\varepsilon}_\mathrm{p}$ represent the strains associated with the elastic and plastic deformation modes. The variables above are also used to represent the corresponding fields in laminar structures, namely mid-surface displacements, equivalent body-forces and stress-resultants and deformations. In geometrically linear models, the equilibrium and compatibility conditions represent conjugate transformations, and operators $\mathbf{D}$ and $\mathbf{D}^*$ are adjoint and linear. In the static boundary condition, matrix $\mathbf{N}$ has for entries the components of the unit outward normal vector associated with the operators listed in the differential operator $\mathbf{D}$.

Equation (5) represents the elastic constitutive relation associating the elastic strain addend $\boldsymbol{\varepsilon}_\mathrm{e}$ with the stress field. Matrix $\mathbf{f}$ is the symmetric, non-singular flexibility matrix of elastic constants characterising a linear, reciprocal elastic law and $\boldsymbol{\varepsilon}_\theta$ represents a residual strain vector.

The description used by Maier and his co-workers, given for instance in Refs. [27–29], is adopted here to model the plastic phase of the constitutive relations. The yield rule (7) is enforced on definition (6) for the finite increment on the plastic potential. Vector $\mathbf{n}$ denotes the unit outward normal to the yield surface, $\varphi_* = 0$, and it is computed using the current values of the stress field in each step of the incremental analysis. The evolution of yield surface is controlled by the selected hardening law, described by parameter h. The flow rule (9) is enforced on the plastic multiplier increments, $\Delta\varepsilon_*$. An associated flow law is assumed in definition (8) for the increments on the plastic deformations, $\Delta\boldsymbol{\varepsilon}_\mathrm{p}$. The vectors of residuals R_φ and $\mathbf{R}_\varepsilon$ collect the nonlinear addends in the definition of plastic potential and plastic deformation increments, respectively.

8. Approximation criteria

In the hybrid-mixed finite element formulation adopted here the stresses $\boldsymbol{\sigma}$, the displacements $\mathbf{u}$ in the domain V and on the static boundary Γ_σ and the increments of the plastic parameters $\Delta\varepsilon_*$ are independently approximated. This is stated by equations (12) to (15), where $\mathbf{S}, \mathbf{U}_V, \mathbf{U}_\Gamma$ and $\mathbf{P}_*$ denote the matrices where the approximation functions associated with the weights listed in arrays $\mathbf{X}, \mathbf{q}_V, \mathbf{q}_\Gamma$ and $\Delta\mathbf{e}^*$ are collected which represent generalised stresses, displacements, and plastic multipliers, respectively:

$$\boldsymbol{\sigma} = \mathbf{S}\mathbf{X} \quad \text{in } V, \tag{12}$$

$$\mathbf{u} = \mathbf{U}_V\mathbf{q}_V \quad \text{in } V, \tag{13}$$

$$\mathbf{u} = \mathbf{U}_\Gamma\mathbf{q}_\Gamma \quad \text{on } \Gamma_\sigma, \tag{14}$$

$$\Delta\boldsymbol{\varepsilon}_* = \mathbf{P}_*\Delta\mathbf{e}_* \quad \text{in } V. \tag{15}$$

A particular feature of the formulation presented here is the use of Walsh series or wavelets to build the stress and displacement approximation matrices $\mathbf{S}, \mathbf{U}_V$ and $\mathbf{U}_\Gamma$. Alternative methods can be used to approximate the plastic multipliers in form (15). A common technique consists in defining a mesh of critical cells where the plastic multipliers are assumed to be constant. When Walsh series are used to approximate the remaining fields, this mesh can be identified with the checkerboard pattern they define, for instance any combination of those illustrated in Fig. 2. In the simulation of the local phenomena associated with plasticity, improved performances have been obtained by subdividing the critical finite elements into cells where the increments on the plastic parameter distribution $\mathbf{P}_*$ are approximated using complete sets of non-negative polynomial functions.

Summarised below are the dual variables associated with generalised stresses $\mathbf{X}$, the generalised displacements in the domain and on the boundary, $\mathbf{q}_V$ and $\mathbf{q}_\Gamma$, and the generalised increments of plastic parameters $\Delta\mathbf{e}_*$; they are, respectively, the generalised strains, e, body-forces, $\mathbf{Q}_V$, tractions, $\mathbf{Q}_\Gamma$, and plastic potentials, $\boldsymbol{\Phi}_*$:

$$\mathbf{e} = \int \mathbf{S}^{\mathrm{T}}\boldsymbol{\varepsilon}\,\mathrm{d}V, \tag{16}$$

$$\mathbf{Q}_V = \int \mathbf{U}_V^{\mathrm{T}}\mathbf{b}\,\mathrm{d}V, \tag{17}$$

$$\mathbf{Q}_\Gamma = \int \mathbf{U}_\Gamma^{\mathrm{T}}\mathbf{t}_\Gamma\,\mathrm{d}\Gamma_\sigma, \tag{18}$$

$$\boldsymbol{\Phi}_* = \int \mathbf{P}_*^{\mathrm{T}}\varphi_*\,\mathrm{d}V. \tag{19}$$

They are so defined as to ensure that the pairs of discrete, dual variables $\{\mathbf{X}, \mathbf{e}\}$, $\{\mathbf{q}_V, \mathbf{Q}_V\}$, $\{\mathbf{q}_\Gamma, \mathbf{Q}_\Gamma\}$, and $\{\Delta\mathbf{e}_*, \Delta\boldsymbol{\Phi}_*\}$ dissipate the same energy as the continuum fields that they represent. It is in consequence of these energy balance requirements, that static-kinematic duality and constitutive reciprocity are preserved in the finite element model defined below. For instance, the following relationship holds for the stress and strain fields:

$$\mathbf{e}^{\mathrm{T}}\mathbf{X} = \int \boldsymbol{\varepsilon}^{\mathrm{T}}\boldsymbol{\sigma}\,\mathrm{d}V$$

9. Finite element relations

The method usually adopted to linearise the yield and flow rules of plasticity consists in replacing the yield surfaces by inscribed polyhedra, while preserving the association condition. The number

of variables and constraints of the problem increases substantially, as pairs of plastic potentials and plastic parameters have to be assigned to each of the yield hyperplanes thus defined. The process adopted here [17], consists in replacing the incremental relations by equivalent asymptotic approximations. The increments on the intervening variables, say $\mathbf{v}$, are expanded in a power series of the form,

$$\Delta \mathbf{v} = \sum_{n=1}^{n=\infty} \mathbf{v}^{(n)} \frac{\tau^n}{n!},$$

where τ denotes an arbitrary non-negative *internal time* parameter, and the same order terms are equated to replace the original nonlinear system by a recursive sequence of equivalent linear complementarity relations. The structure of the resulting sequence of equations and inequations is identical to system (1–11) with every incremental variable $\Delta \mathbf{v}$ and residual $\mathbf{R}$ being replaced by their n-th order derivatives, $\mathbf{v}(n)$ and $\mathbf{R}(n)$. The resulting system is recursive because the n-th order residuals $\mathbf{R}(n)$ depend on variables of order lower than the n-th.

The finite element relations are obtained by combining the relations (1) to (19), after applying the standard perturbation technique described above. The resulting relations are listed below, where the n-th derivative notation is dropped to simplify the presentation:

$$\begin{bmatrix} -\mathbf{A}_V^{\mathrm{T}} \\ \mathbf{A}_\Gamma^{\mathrm{T}} \end{bmatrix} \mathbf{X} = \begin{Bmatrix} \mathbf{Q}_V \\ \mathbf{Q}_\Gamma \end{Bmatrix}, \tag{20}$$

$$\mathbf{e}_* + \mathbf{e}_{\mathrm{p}} - \mathbf{e}_\Gamma = \begin{bmatrix} -\mathbf{A}_V & \mathbf{A}_\Gamma \end{bmatrix} \begin{Bmatrix} \mathbf{q}_V \\ \mathbf{q}_\Gamma \end{Bmatrix}. \tag{21}$$

$$\mathbf{e}_{\mathrm{e}} = \mathbf{F}\mathbf{X} + \mathbf{e}_\theta, \tag{22}$$

$$\boldsymbol{\Phi}_* = -\mathbf{H}_* e_* + \mathbf{N}_*^{\mathrm{T}} \mathbf{X} + \mathbf{R}_\Phi^*, \tag{23}$$

$$\boldsymbol{\Phi}_* + \Delta \boldsymbol{\Phi}_* \leq \mathbf{0}, \tag{24}$$

$$\mathbf{e}_{\mathrm{p}} = \mathbf{N}_* \mathbf{e}_* + \mathbf{R}_{\mathrm{e}}^*, \tag{25}$$

$$\Delta \mathbf{e}_* \geq \mathbf{0}, \tag{26}$$

$$\boldsymbol{\Phi}_*^{\mathrm{T}} \Delta \mathbf{e}_* = 0, \tag{27}$$

$$\Delta \boldsymbol{\Phi}_*^{\mathrm{T}} \Delta \mathbf{e}_* = 0. \tag{28}$$

To obtain the discrete description (20) for Statics, the equilibrium and the static boundary conditions (1) and (3) are inserted in definitions (17) and (18) for the generalised body-forces and tractions, respectively. The stress approximation (12) is enforced next in the resulting equations, to yield:

$$\mathbf{A}_V = \int (\mathbf{D}\mathbf{S})^{\mathrm{T}} \mathbf{U}_V \, \mathrm{d}V, \tag{29}$$

$$\mathbf{A}_\Gamma = \int (\mathbf{N}\mathbf{S})^{\mathrm{T}} \mathbf{U}_\Gamma \, \mathrm{d}\Gamma_\sigma. \tag{30}$$

To derive the dual description (21) of Kinematics, the compatibility condition (2) is first substituted in definition (16) for the generalised strains and integrated by parts to mobilise the boundary terms. The displacement approximation (13) is inserted in the domain integral present in the resulting equation, while the boundary integral term is uncoupled into the static and kinematic portions

to enforce the kinematic boundary conditions (4) and the boundary displacement approximation (14), respectively. Definitions (29) and (30) are recovered and the following expression is found for the generalised strains associated with the prescribed displacements:

$$\mathbf{e}_\Gamma = \int (\mathbf{NS})^{\mathrm{T}} \mathbf{u}_\Gamma \, \mathrm{d}\Gamma_u. \tag{31}$$

The discrete description of elasticity (22) is obtained by substituting the local condition (5) in definition (16) for the generalised strains and eliminating next the stress field using the approximation condition (12), to yield:

$$\mathbf{F} = \int \mathbf{S}^{\mathrm{T}} \mathbf{f} \, \mathbf{S} \, \mathrm{d}V, \tag{32}$$

$$\mathbf{e}_\theta = \int \mathbf{S}^{\mathrm{T}} \boldsymbol{\varepsilon}_\theta \, \mathrm{d}V. \tag{33}$$

Definition (23) for the generalised plastic potentials is derived by inserting in definition (19) the plastic potential equation (6), together with the approximations (12) and (15) for the stress and plastic parameter fields. The definition for the plastic addend of the generalised strains is obtained by substituting the plastic parameter approximation (15) in definition (16) written for the plastic strains (8). The following expressions are thus found for the finite element plasticity arrays:

$$\mathbf{H}_* = \int \mathbf{P}_*^{\mathrm{T}} h \mathbf{P}_* \, \mathrm{d}V, \tag{34}$$

$$\mathbf{N}_* = \int \mathbf{S}^{\mathrm{T}} \mathbf{n} \mathbf{P}_* \, \mathrm{d}V, \tag{35}$$

$$\mathbf{R}_\Phi^* = \int \mathbf{P}_*^T \mathbf{R}_\varphi \, \mathrm{d}V, \tag{36}$$

$$\mathbf{R}_{\mathrm{e}}^* = \int \mathbf{S}^{\mathrm{T}} \mathbf{R}_\varepsilon \, \mathrm{d}V. \tag{37}$$

The results summarised above show that duality holds both in the description for Statics and Kinematics, stated by equations (20) and (21), and in the description for the static and kinematic phases of plasticity, defined by equations (23) and (25). Moreover, and according to definitions (32) and (34), constitutive reciprocity holds as the flexibility and hardening matrices are symmetric.

Based on the same results, it is possible to verify that equations (20) represent the $\mathbf{U}_V$- and the $\mathbf{U}_\Gamma$-weighed residual enforcement respectively of the equilibrium and static boundary conditions (1) and (3). Similarly, equations (21) and (22) represent the $\mathbf{S}$-weighed residual enforcement of the compatibility and elasticity relations (2) and (5), respectively. The same interpretation holds for relation (25) concerning now the finite element representation of the flow rule defined by condition (8). Lastly, relations (23) and (24) can be interpreted as the $\mathbf{P}_*$-weighed enforcement of the yield rule defined by conditions (6) and (7).

10. Governing system

The elementary governing system (38) is obtained by combining the incremental discrete description of statics, kinematics, elasticity and plasticity and eliminating next as explicit variables the elastic and plastic addends of generalised strains:

$$\begin{bmatrix} \mathbf{F} & \mathbf{A}_V & -\mathbf{A}_\Gamma & \mathbf{N}_* \\ \mathbf{A}_V^{\mathrm{T}} & \mathbf{0} & \mathbf{0} & \mathbf{0} \\ -\mathbf{A}_\Gamma^{\mathrm{T}} & \mathbf{0}^{\mathrm{T}} & \mathbf{0} & \mathbf{0} \\ \mathbf{N}_*^{\mathrm{T}} & \mathbf{0}^{\mathrm{T}} & \mathbf{0}^{\mathrm{T}} & -\mathbf{H}_* \end{bmatrix} \begin{Bmatrix} \mathbf{X} \\ \mathbf{q}_V \\ \mathbf{q}_\Gamma \\ \mathbf{e}_* \end{Bmatrix}^{(n)} = \begin{Bmatrix} \mathbf{e}_\Gamma - \mathbf{e}_\theta - \mathbf{R}_{\mathrm{e}}^* \\ -\mathbf{Q}_V \\ -\mathbf{Q}_\Gamma \\ \mathbf{\Phi}_* - \mathbf{R}_\Phi^* \end{Bmatrix}^{(n)}, \tag{38a-d}$$

$$\mathbf{\Phi}_* + \Delta\mathbf{\Phi}_* \leq 0, \quad \Delta\mathbf{e}_* \leq 0, \quad \mathbf{\Phi}_*^{\mathrm{T}}\Delta\mathbf{e}_* = 0, \quad \Delta\mathbf{\Phi}_*^{\mathrm{T}}\Delta\mathbf{e}_* = 0. \tag{38e-h}$$

The system governing the response of the finite element mesh is obtained by assembling the elementary equations (38) simply by requiring neighbouring elements to share the same boundary displacement approximation law (14). The structure of the resulting system is similar to that of system (38). The assembling of this system is straightforward as all variables are strictly element dependent, except for the generalised boundary displacements which can be shared by two adjacent elements. It is strictly a direct allocation procedure without the summations typical of the conventional finite element formulation.

Because the interelement continuity conditions are implemented in terms of boundary tractions, through definition (18) and equation (20b), this model is termed a *hybrid-mixed stress* model. In the complementary *hybrid-mixed displacement* model [1] it is the boundary tractions that are approximated, instead of the boundary displacements, and the traction approximation functions are then used to enforce interelement displacement continuity conditions.

To obtain the system of equations governing the response of elastic systems, it suffices to eliminate in system (38) all the variables and arrays associated with the plastic phase of the response. Similarly, to perform a rigid-plastic analysis, system (38) can still be used by setting to zero the intervening elastic operators, as illustrated, for instance, in Ref. [31].

11. ENERGY STATEMENTS

Because the finite element formulations are so often derived from energy statements, it is of interest to illustrate how these statements can be obtained *a posteriori* for a formulation derived from the fundamental structural relations, as in the present case. This can be easily achieved using mathematical programming equivalence theory, as it has been suggested by different authors [31, 32]. In the present context, the basic technique consists in interpreting system (38) as a symmetric linear complementarity problem and derive the associated pair of dual quadratic programs using the Karush-Kuhn-Tucker equivalence conditions.

Programs (39) and (40) are obtained by choosing the primal and dual constraint sets to identify with the (average) static admissibility conditions (38b) to (38e) and kinematic admissiblity conditions (38a) and (38f), respectively:

$$\text{Min } z_* = \tfrac{1}{2}\mathbf{X}^{\mathrm{T}}\mathbf{F}\mathbf{X} + \tfrac{1}{2}\mathbf{e}_*^{\mathrm{T}}\mathbf{H}_*\mathbf{e}_* - \mathbf{X}^{\mathrm{T}}(\mathbf{e}_\Gamma - \mathbf{e}_\theta - \mathbf{R}_{\mathrm{e}}^*) \tag{39a}$$

$$\text{subject to constraints:} \quad \mathbf{A}_V^{\mathrm{T}}\mathbf{X} = -\mathbf{Q}_V, \quad \mathbf{A}_\Gamma^{\mathrm{T}}\mathbf{X} = \mathbf{Q}_\Gamma, \quad \mathbf{H}_*\mathbf{e}_* - \mathbf{N}_*^{\mathrm{T}}\mathbf{X} \geq \mathbf{R}_\Phi^*, \tag{39b-d}$$

$$\text{Min } z = \tfrac{1}{2}\mathbf{X}^{\mathrm{T}}\mathbf{F}\mathbf{X} + \tfrac{1}{2}\mathbf{e}_*^{\mathrm{T}}\mathbf{H}_*\mathbf{e}_* - \mathbf{q}_V^{\mathrm{T}}\mathbf{Q}_V - \mathbf{q}_\Gamma^{\mathrm{T}}\mathbf{Q}_\Gamma - \mathbf{e}_*^{\mathrm{T}}\mathbf{R}_\Phi^* \tag{40a}$$

$$\text{subject to constraints:} \quad \mathbf{F}\mathbf{X} + \mathbf{A}_V\mathbf{q}_V - \mathbf{A}_\Gamma\mathbf{q}_\Gamma + \mathbf{N}_*\mathbf{e}_* = \mathbf{e}_\Gamma - \mathbf{e}_\theta - \mathbf{R}_{\mathrm{e}}^*, \quad \mathbf{e}_* \geq \mathbf{0}. \tag{40b-c}$$

Using the expressions given above for the finite element arrays in the definitions for the objective functions z and z_* and enforcing next the finite element approximations (12) to (15), it is found

that they identify with the potential complementary energy and the potential energy of the system, U_* and U respectively:

$$z_* = U_* = E_* - W_*,$$

$$z = U = E - W,$$

$$E_* = \frac{1}{2}\int \boldsymbol{\sigma}^{\mathrm{T}}(\boldsymbol{\varepsilon}_{\mathrm{e}} + \boldsymbol{\varepsilon}_\theta + 2\mathbf{R}_\varepsilon)\,\mathrm{d}V + \frac{1}{2}\int \boldsymbol{\varepsilon}_*^{\mathrm{T}} h\boldsymbol{\varepsilon}_*\,\mathrm{d}V,$$

$$E = \frac{1}{2}\int \boldsymbol{\sigma}^{\mathrm{T}}(\boldsymbol{\varepsilon}_{\mathrm{e}} - \boldsymbol{\varepsilon}_\theta)\,\mathrm{d}V + \frac{1}{2}\int \boldsymbol{\varepsilon}_*^{\mathrm{T}}(h\boldsymbol{\varepsilon}_* - 2\mathbf{R}_\varphi)\,\mathrm{d}V,$$

$$W_* = \int \mathbf{u}^{\mathrm{T}}\mathbf{b}\,\mathrm{d}V + \int \mathbf{u}^{\mathrm{T}}\mathbf{t}_\Gamma\,\mathrm{d}\Gamma_\sigma,$$

$$W = \int \mathbf{t}^{\mathrm{T}}\mathbf{u}_\Gamma\,\mathrm{d}\Gamma_u.$$

Therefore, program (39) represents the stationary theorem of Haar-Karman and program (40) the dual Hodge-Kachanov statement. Different identifications for the primal-dual constraint set generate alternative energy statements. For instance, the (non-dual) programs below can be obtained by so choosing the constraint sets as to identify either with the yield or the flow rules of plasticity:

$$\text{Max } w_* = -\tfrac{1}{2}\mathbf{X}^{\mathrm{T}}\mathbf{F}\mathbf{X} - \tfrac{1}{2}\mathbf{e}_*^{\mathrm{T}}\mathbf{H}_*\mathbf{e}_* - \mathbf{q}_V^{\mathrm{T}}(\mathbf{A}_V^{\mathrm{T}}\mathbf{X} + \mathbf{Q}_V) - \mathbf{q}_\Gamma^{\mathrm{T}}(\mathbf{A}_\Gamma^{\mathrm{T}}\mathbf{X} - \mathbf{Q}_\Gamma) + \mathbf{X}^{\mathrm{T}}(\mathbf{e}_\Gamma - \mathbf{e}_\theta - \mathbf{R}_{\mathrm{e}}^*),$$

$$\text{subject to constraints:} \quad \mathbf{H}_*\mathbf{e}_* - \mathbf{N}_*^{\mathrm{T}}\mathbf{X} \geq \mathbf{R}_\Phi^*,$$

$$\text{Min } w = -\tfrac{1}{2}\mathbf{X}^{\mathrm{T}}\mathbf{F}\mathbf{X} + \tfrac{1}{2}\mathbf{e}_*^{\mathrm{T}}\mathbf{H}_*\mathbf{e}_* - \mathbf{q}_V^{\mathrm{T}}(\mathbf{A}_V^{\mathrm{T}}\mathbf{X} + \mathbf{Q}_V) + \mathbf{q}_\Gamma^{\mathrm{T}}(\mathbf{A}_\Gamma^{\mathrm{T}}\mathbf{X} - \mathbf{Q}_\Gamma) + \mathbf{X}^{\mathrm{T}}(\mathbf{e}_\Gamma - \mathbf{e}_\theta - \mathbf{R}_{\mathrm{e}}^*)$$
$$-\mathbf{e}_*^{\mathrm{T}}(\mathbf{N}_*^{\mathrm{T}}\mathbf{X} + \mathbf{R}_\Phi^*),$$

$$\text{subject to constraints:} \quad \mathbf{e}_* \geq \mathbf{0}.$$

Back-substitution yields the following definition for the optimisation functionals, which shows that the programs above relate with the Hellinger-Reissner statement associated with the hybrid-mixed stress model in use:

$$w = w_* = -U_* - \int \mathbf{u}^{\mathrm{T}}(\mathbf{D}\boldsymbol{\sigma} + \mathbf{b})\,\mathrm{d}V + \int \mathbf{u}^{\mathrm{T}}(\mathbf{t} - \mathbf{t}_\Gamma)\,\mathrm{d}\Gamma_\sigma.$$

An equally interesting application of mathematical programming is the derivation of criteria for the existence, uniqueness and stability of the finite element solutions. Different applications are reported in Refs. [31, 32].

12. Incremental analysis

The programs stated above, in particular those involving a low number of constraints, can be used to perform elastoplastic deformation analyses using appropriate mathematical programming algorithms. However, the incremental methods of elastoplastic analysis are more frequently used in practical applications because of the advantages they offer, both in terms of additional information and computational efficiency.

The incremental process is usually based on a pre-selected load or displacement parameter. To avoid the permanent assessment of the monotonicity of the controlling term, the perturbation

parameter is identified with the increment of the external work rate, $\tau = \Delta\overline{W}$, and used to control the incremental process. Here, to implement the incremental elastoplastic process, it is assumed, for simplicity, that the applied tractions are piecewise proportional to a load parameter λ, to yield the following definitions for the generalised boundary traction resultants and the associated external work rate:

$$\mathbf{t}_\Gamma = \bar{\mathbf{t}}_\Gamma \lambda \quad \text{on } \Gamma_\sigma,$$

$$\mathbf{Q}_\Gamma = \mathbf{a}\lambda,$$

$$\Delta\overline{W} = \mathbf{a}^{\mathrm{T}} \Delta\mathbf{q}_\Gamma,$$

$$\mathbf{a} = \int \mathbf{U}_\Gamma^{\mathrm{T}} \bar{\mathbf{t}}_\Gamma \, \mathrm{d}\Gamma_\sigma.$$

The solving system is thus replaced by the following restricted basis linear programming problem:

Maximise $\Delta\overline{W}$ subject to constraints: (41a)

$$\begin{bmatrix} \mathbf{F} & \mathbf{A}_V & -\mathbf{A}_\Gamma & \mathbf{N}_* & \mathbf{0} \\ \mathbf{A}_V^{\mathrm{T}} & \mathbf{0} & \mathbf{0} & \mathbf{0} & \mathbf{0} \\ -\mathbf{A}_\Gamma^{\mathrm{T}} & \mathbf{0}^{\mathrm{T}} & \mathbf{0} & \mathbf{0} & \mathbf{a} \\ \mathbf{N}_*^{\mathrm{T}} & \mathbf{0}^{\mathrm{T}} & \mathbf{0}^{\mathrm{T}} & -\mathbf{H}_* & \mathbf{0} \\ \mathbf{0}^{\mathrm{T}} & \mathbf{0}^{\mathrm{T}} & \mathbf{a}^{\mathrm{T}} & \mathbf{0}^{\mathrm{T}} & 0 \end{bmatrix} \begin{Bmatrix} \mathbf{X} \\ \mathbf{q}_V \\ \mathbf{q}_\Gamma \\ \mathbf{e}_* \\ \lambda \end{Bmatrix}^{(n)} = \begin{Bmatrix} -\mathbf{R}_{\mathrm{e}}^* \\ \mathbf{0} \\ \mathbf{0} \\ \mathbf{\Phi}_* - \mathbf{R}_\Phi^* \\ \overline{W} \end{Bmatrix}^{(n)}, \tag{41b-f}$$

$$\mathbf{\Phi}_* + \Delta\mathbf{\Phi}_* \leq \mathbf{0}, \quad \Delta\mathbf{e}_* \geq \mathbf{0}, \quad \mathbf{\Phi}_*^{\mathrm{T}} \Delta\mathbf{e}_* = 0, \quad \Delta\mathbf{\Phi}_*^{\mathrm{T}} \Delta\mathbf{e}_* = 0. \tag{41g-j}$$

A similar procedure can be applied to other loading terms assumed constant in system (38), namely the body-forces, the prescribed displacements or the residual strains.

The numerical results presented below are obtained by implementing the governing system in form (41) and, also, by applying an alternative technique very common in the hybrid element applications, consisting in the pre-condensation of the governing system (38) at element level by direct elimination of the generalised stresses and displacements $\mathbf{X}$ and $\mathbf{q}_V$. An important reduction in the number of explicit degrees of freedom is thus gained as the boundary displacements $\mathbf{q}_\Gamma$ and the plastic multipliers $\mathbf{e}_*$, besides the load parameter λ, are the only variables present in the solving system. Pre-condensation of all variables associated with the elastic phase is also possible and frequently used. However, and as it is illustrated below, this is achieved at the expense of a substantially lower sparsity index for the solving system, which may require a storage capacity of the same magnitude of system (41). Moreover, this technique complicates the implementation of adaptive techniques and therefore wastes one of the most interesting features of the formulation, its natural ability to support coarse meshes based on p-adaptive elements.

13. Numerical implementation

The example chosen to illustrate the performance of the stress model of the hybrid-mixed finite element formulation based on Walsh functions and wavelets is the simply supported beam subject to a uniform distributed load, shown in Fig. 7. The vertical displacements at the end-sections are constrained and the simplification of symmetry is used in the computations.

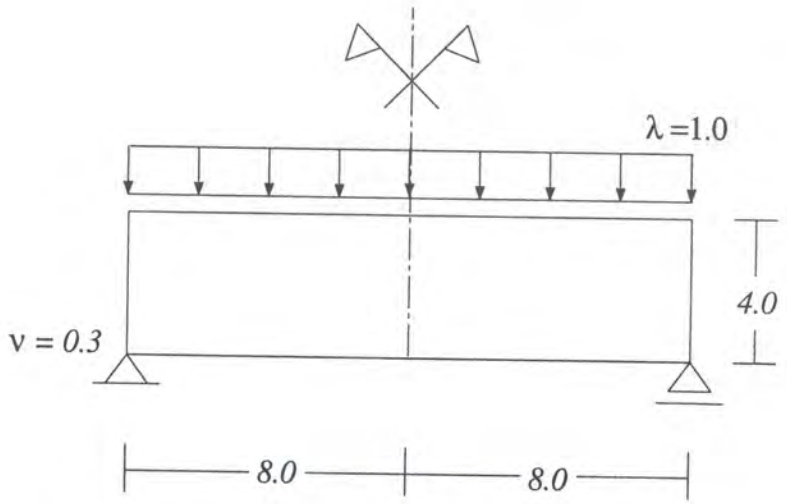

Fig. 7. The simply supported beam subject to a uniform transverse load.

This example is selected because the elastic and elastoplastic responses of this two-dimensional structure are well known and familiar to the readers. The Walsh approximation is used to illustrate all phases in the numerical implementation of the elastic response. The structural response thus obtained is compared with the solution generated by the wavelet approximation, which is later used to generate the estimate for the elastoplastic response.

Both the p- and h-refinement techniques are applied to test the Walsh function solutions. The degree p of the functions ranges from 2 to 6 and four discretisation meshes are used, with 1, 2, 4 and 16 regular elements, as shown in Fig. 8. The stresses and the displacements in the domain are interpolated in each element using 2^p and 2^{p-1} Walsh functions, respectively; the boundary displacements are approximated with $2^p - 1$ functions.

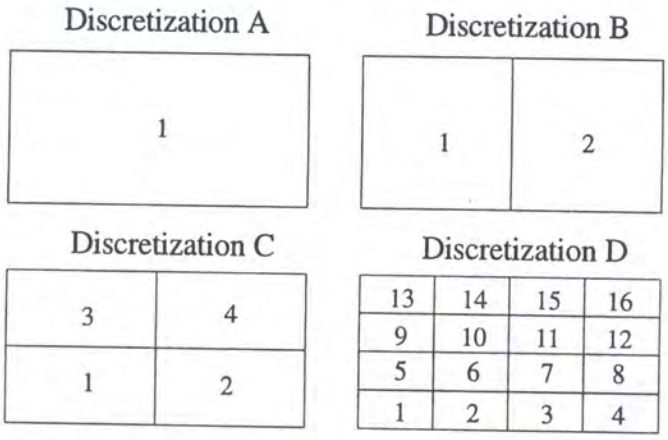

Fig. 8. Finite element meshes adopted in the numerical tests.

13.1. Pre-Processing

One of the interesting features of the Walsh functions and wavelets is that they can be used to construct hierarchical series. This allows for the development of very rich, p-enriched elements and the use of coarse finite element meshes. Also, the amount of information needed to characterise the

yield surface is minimised by the asymptotic description adopted for the plasticity relations. Gains at pre-processing level derive essentially from these two facts. The data structure is small in dimension and dependency on efficient meshing algorithms is greatly reduced. Parallel implementation is simplified as few elements need to be handled.

These aspects are well illustrated by the example under analysis. The information to be fed and stored covers, essentially, the co-ordinates of the nodes necessary to define the geometry of the structure, the data on the topography of the mesh (assignment of sides to the nodes and of elements to the sides), the static and kinematic boundary conditions, the relevant material constants and the approximation criteria in each finite element.

13.2. Computation of the Structural Matrices

The use of Walsh series and wavelets to approximate the structural fields has a direct impact on the computational costs related with the generation of the approximation functions, the determination of the structural operators and the maximisation of their sparsity indices. Speed in the generation of these functions derives from their digital nature and the high sparsity indices are consequent upon orthogonality.

The properties the Walsh series enjoy can be exploited to establish closed-form solutions to the integral expressions of the structural matrices [20, 22]. Numerical integration is thus avoided, reducing substantially the computation times. From a multiprocessing standpoint, it is seen that the major advantage the hybrid-mixed formulation offers is, again, the possibility of using a very small number of hierarchical elements. Similar gains are offered by wavelets. However, when part of the intersection of the different wavelets used in the approximation lies outside the domain considered, orthogonality disappears and for that case a numerical integration rule must be used.

The number of degrees of freedom, N, involved in the Walsh approximation of the example under consideration obtained for the governing system (38) specialised for the elastic analysis are given in Table 3. Given in the same table are the values obtained by condensing system (38) in the generalised boundary displacements $\mathbf{q}_\Gamma$. The information summarised in Table 3 shows that the Walsh approximation induces a rapid increase in the dimension of the solving system, thus stressing the need to find the appropriate balancing of the p- and h-refinement techniques. A substantial reduction in the number of degrees of freedom is obtained by condensing the system in the boundary displacement variables.

Table 3. Degree of freedom, N, for the elastic tests with the Walsh functions.

Mesh	System	p = 2	3	4	5	6
1×1	Full	74	266	986	3.770	14.714
	Condensed	18	42	90	186	378
1×2	Full	148	532	1.972	7.540	29.428
	Condensed	36	84	180	372	756
2×2	Full	284	1.036	3.884	14.956	58.604
	Condensed	60	140	300	620	1.260
4×4	Full	1.112	4.088	15.416	59.576	233.912
	Condensed	216	504	1.080	2.232	4.536

It is important to point out that the numbers given in Table 3 cannot be used directly to judge the numerical performance of either of the techniques. As it is shown below, accurate solutions can be obtained with the lower level p and h approximations; the more refined discretisations are used here to illustrate the handling of large sparse systems. The implementation of the very large,

full systems can be performed at high speed and can remain competitive when compared with the condensed form, with the added advantage of being well suited to host the enforcement of adaptive procedures.

The time spent in setting up the full governing system when the Walsh approximation is used with the alternative discretisations being tested is given in Table 4. These results show that the time spent in reading the data and in computing and storing the finite element matrices is always very small, both in absolute value and when compared with the total computation time, as it is shown below.

Table 4. Time (second) spent in the pre-processing phase (elastic tests with Walsh approximation and full systems).

Mesh	p = 2	3	4	5	6
1×1	0.01	0.02	0.02	0.06	0.32
1×2	0.01	0.02	0.02	0.09	0.68
2×2	0.02	0.02	0.05	0.21	1.29
4×4	0.05	0.08	0.17	0.75	5.13

13.3. Storage of the Governing System

Sparse matrix storage and solution techniques must be used with hybrid-mixed formulations to exploit the high sparsity indices that can be achieved. This is well illustrated in Fig. 9 which shows the typical pattern of the coefficient matrix in the system governing the elastic response of the problem under analysis when the 2 × 2 mesh is used. It is obtained using the *SMMS* package developed by Alvarado [33]; black and white zones represent non-zero and zero coefficients, respectively.

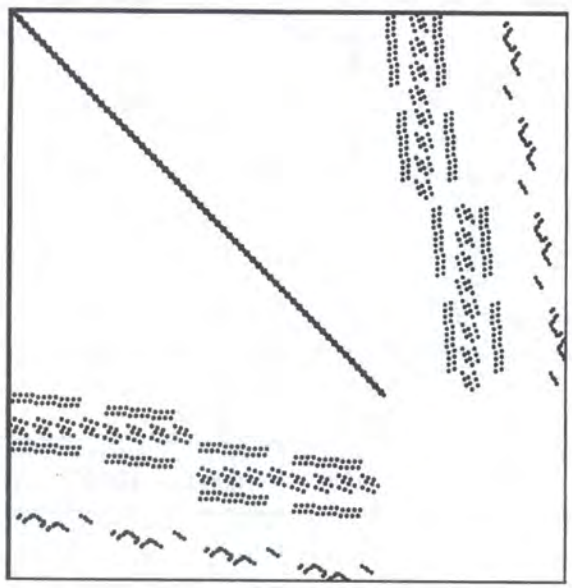

Fig. 9. Typical pattern of the coefficient matrix.

The sparsity indices, η, obtained for the governing system (38) specialised for the elastic analysis of the simply supported beam based on the Walsh functions are shown in Figs. 10 and 11 for the

condensed and full formats, respectively. The sparsity index represents the ratio between the number of zero coefficients and the total number of entries of the system matrix, N^2.

The results given in Figs. 10 and 11 show that very high sparsity indices are always obtained with the Walsh approximation. The reduction in the number of degrees of freedom obtained for the condensed system is achieved at the expense of poorer sparsity indices. The traditional finite element storage methods, such as the half-bandwidth and skyline schemes, are inappropriate for hybrid-mixed formulations as they lead to the storage of a large number of zero coefficients and the amount of memory required and the CPU time spent in the calculations becomes prohibitive.

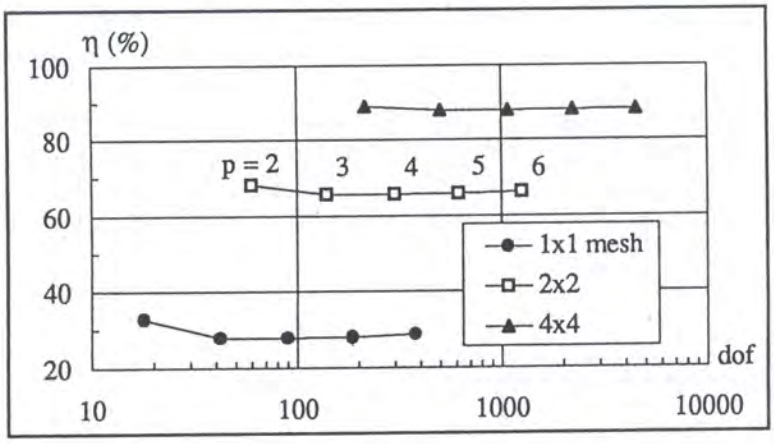

Fig. 10. Sparsity index for the condensed system.

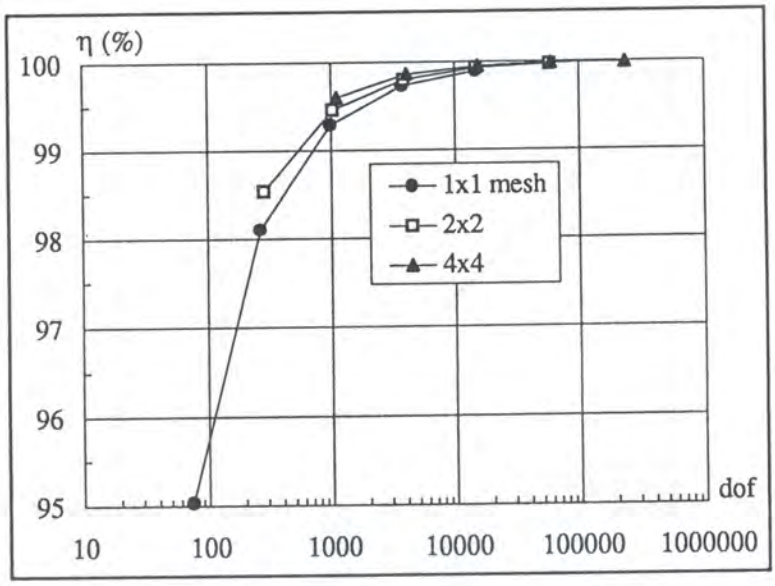

Fig. 11. Sparsity index for the full system.

Two alternative data structures have been used and tested [21]. In the *co-ordinate scheme* [34], the non-zero coefficients are stored in the form of an ordered set of triples (a_{mn}, m, n). It is simple to implement and well suited to be used in scalar machines when coupled with iterative system solvers. Its major limitation is the difficulty to access directly by rows or columns. In the *sparse row-wise*

format [18], one of the most commonly used storage schemes for sparse matrices, the values of the non-zero coefficients are stored by rows, along with their column indices, in two arrays. An array of pointers is also used to indicate where the description of each row begins. This data structure can be adapted to achieve a dense and convenient representation for symmetric matrices with non-zero diagonal elements. Direct access by rows is simple. The sparse row-wise format is particularly well suited when direct methods are used to solve the system of equations.

13.4. Solution of the Governing System

The procedure used to solve the incremental elastoplastic problem (41) is described in general terms in Ref. [35] and specialised in Ref. [17] to nonlinear elastoplastic analysis of frame structures. The algorithm is based on a direct extension of the simplex method. In each increment, system (41) is solved for the currently active yield modes and the step length is automatically adjusted to detect and implement plastic straining and unstressing and also to control the accumulation of errors due to the truncation of the power series expansion. This solution scheme relies heavily on the sequential solution of sparse systems of linear equations. The supporting solver should be so designed as to store and operate only the non-zero coefficients to avoid the redundant operations involving zero entries. At the same time, sparsity should be preserved as much as possible by minimising fill-in, that is the transformation of zero coefficients in the initial system into non-zero coefficients during the implementation of the solution procedure.

Both direct and iterative system solvers have been used in the implementation of the formulation reported here [21]. The *direct solvers* tested, based on Gauss elimination, are Pissanetzky's scheme [18], and the multifrontal solution scheme suggested by Duff and Reid [36] encoded in routine *MA47* of Harwell Subroutine Library [37]. The *iterative solvers* that have been tested are based on the conjugate gradient method with different preconditioning schemes: diagonal pre-conditioning, CG_D, symmetric successive over relaxation, CG_SSOR, and incomplete factorisation, CG_IF.

The iterative methods are very attractive in what regards minimisation of computer storage requirements. Usually, their implementation requires only the storage of the initial coefficient matrix, the right-hand side vector, the solution vector, and one or two working vectors. However, they are sensitive to the alternative stopping criteria and the number of iterations necessary to obtain a suitable solution is unknown *a priori*. On the other hand, the direct methods provide the solution after a finite number of operations is performed but are very sensitive to fill-in. They seem to be particularly convenient when several systems of equations sharing the same coefficient matrix, or at least the same non-zero pattern distribution, are to be solved.

Shown in Fig. 12 are the solution times obtained for the elastic tests under analysis when the direct and iterative solvers are used. It is seen that both direct methods perform well. The method of Duff and Reid becomes significantly more competitive as the dimension of the system increases because in Pissanetzky's scheme fill-in is not optimised. In fact, it crashed for the 2×2 mesh with $p = 6$ due to insufficient memory induced by fill-in. The best results are obtained with the incomplete factorisation scheme, CG_IF, which compares favourably with respect to the direct methods. The differences in relative performance found for the remaining versions of the iterative solver are not relevant. The number of iterations and the corresponding execution times are given in Fig. 13. The results shown in Figs. 12 and 13 relate to the Walsh approximation on the elastic test with the 2×2 mesh and $2 \leq p \leq 6$.

To improve the performance, the system at element level is condensed using Pissanetzky's scheme and the assembled system is solved with Duff and Reid's method, the same adopted to solve the full system. As the results given in Table 5 show, pre-condensation is competitive when meshes with a significant number of identical elements are used, a situation that may not occur frequently with hybrid-mixed formulations, which are usually implemented on coarse meshes of relatively few macroelements.

The experience with parallel processing is still too limited to advance with substantive comments. However, it seems to be important to exploit the low-level, highly localised element linkage, which

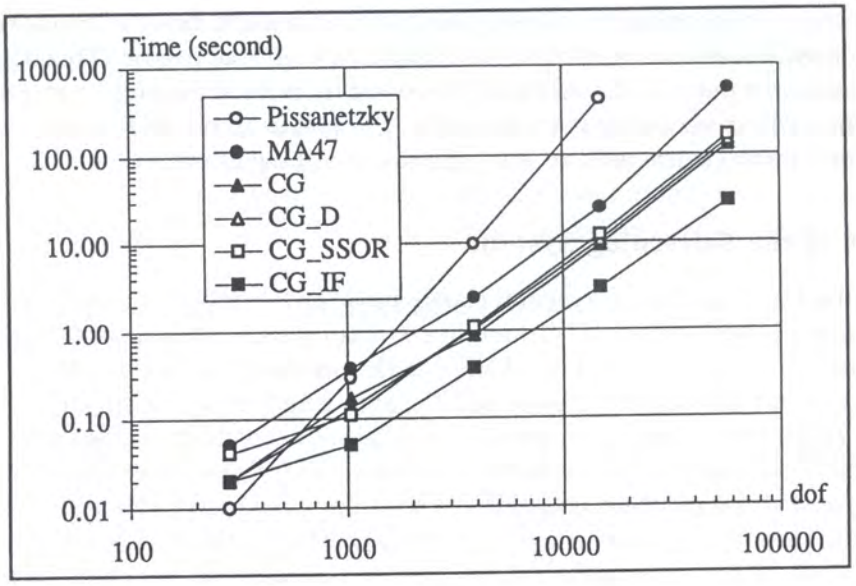

Fig. 12. Solution times for the full system.

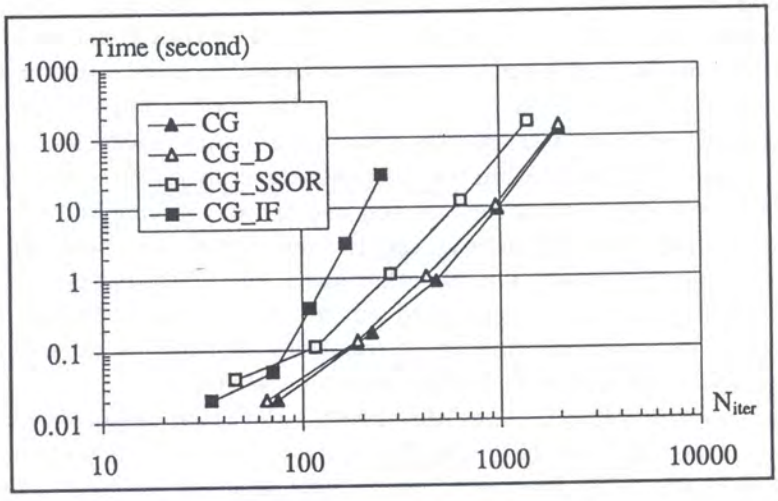

Fig. 13. Number of iterations for the full system.

Table 5. Solution time (seconds) of the governing system in full and condensed forms (elastic tests with Walsh approximation and MA47 routine).

Mesh	System	p = 2	3	4	5	6
1×1	Condensed	0.05	0.11	0.85	13.64	276.70
	Full	0.03	0.06	0.44	4.80	113.80
2×2	Condensed	0.03	0.11	1.05	14.35	287.18
	Full	0.05	0.37	2.37	24.65	538.18

is solely dependent on the boundary approximation functions. In system (41), the boundary displacements $\mathbf{q}_\Gamma$ are the only variables that can be shared by two elements. The variables defining the stress, displacement and plastic multiplier fields are strictly element dependent.

13.5. Post-Processing

In the hybrid-mixed formulations the representation of the stress, displacement and plastic multiplier fields is immediate as these fields are directly approximated. After solving the governing system, the different fields are computed from the independent approximations, as stated by Eqs. (12) to (15), and the results are fed into a graphic interface developed locally [38]. The fast transformation techniques play an important role at this stage. Also, parallelisation of post-processing at element level is immediate as the relevant variables are element dependent and no smoothing needs to be performed.

The post-processing times obtained in a sequential processing mode are given in Table 6. These values represent the time spent to compute and represent graphically all the components of the three fields approximated directly, using Eqs. (12) to (14). In each finite element, these values are computed in each of the cells defining the Walsh checkerboard approximation pattern.

Table 6. Time (seconds) spent in the post-processing phase (elastic tests with Walsh approximation).

Mesh	p = 2	3	4	5	6
1×1	0.02	0.02	0.12	0.48	3.12
1×2	0.03	0.09	0.22	1.09	5.95
2×2	0.06	0.14	0.52	2.41	13.23
4×4	0.14	0.47	2.02	9.19	59.09

The total time spent in the analysis, including pre-processing, solution of the governing system and post-processing, is given in Table 7 for the most representative tests reported above. The results assigned to the *MA47* and *CG_IF* routines are obtained for the full, non-condensed system. The computation times for the condensed system correspond to the combination of Pissanetzky's and Duff and Reid's schemes described above.

Table 7. Total time (seconds) spent in the analysis (elastic tests with Walsh approximation).

Mesh	Scheme	p = 2	3	4	5	6
1×1	*MA47*	0.06	0.10	0.58	5.34	117.24
	CG_IF	0.05	0.09	0.51	3.59	32.60
	Condensed	0.08	0.15	0.99	14.18	280.14
2×2	*MA47*	0.13	0.53	2.94	27.27	552.70
	CG_IF	0.15	0.59	3.34	24.91	220.03
	Condensed	0.11	0.27	1.62	16.97	301.70

It is worth recalling that the dimension of the condensed system ranges from 18 to 756 degrees of freedom; the corresponding values for the full system are 74 and 29.428. The performance is good in global terms but the values given in the table above show the importance of combining conveniently the p- and h-refinements with the most appropriate solver, while weighing the importance of storage requirements, in particular due to fill-in, with the consequences of coupling the solution procedure with adaptive techniques.

14. Simulation of the structural response

The convergence of the Walsh elastic solution, both in terms of the strain energy, E, and of the vertical displacement at mid-span, δ, computed from the domain approximation, is shown in Figs. 14 and 15, respectively. The solutions are normalised with respect to the values obtained through

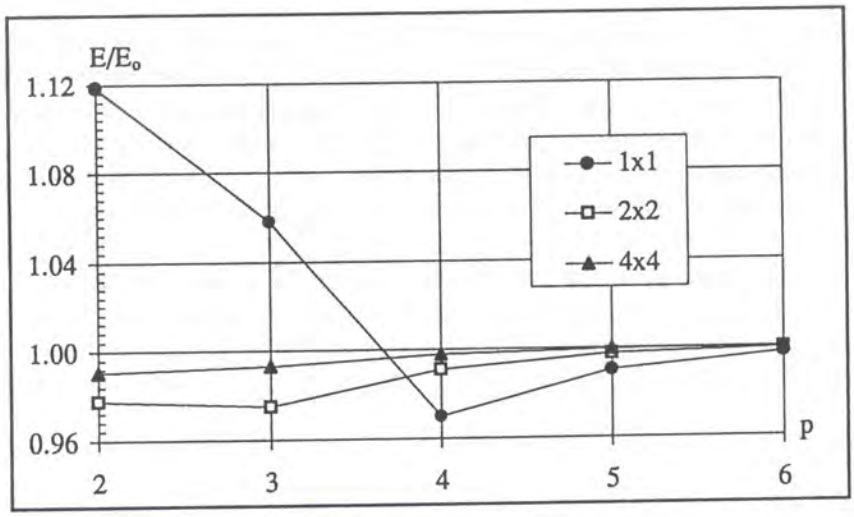

Fig. 14. Convergence of the normalised strain energy.

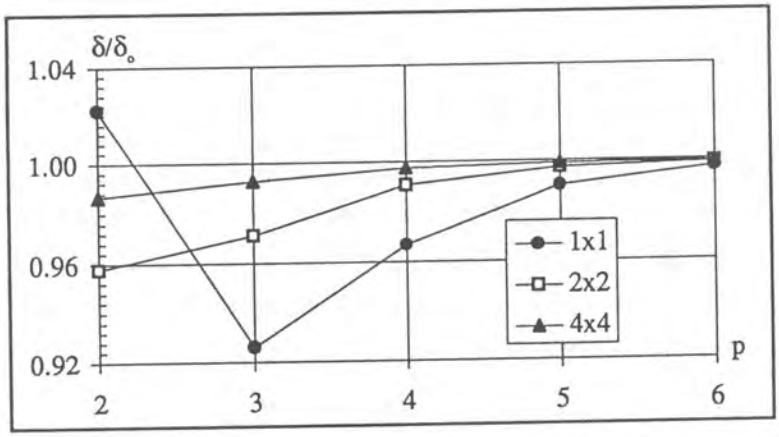

Fig. 15. Convergence of the normalised vertical displacement.

Timoshenko's beam theory $E_0 = 466.86$ and $\delta_0 = 178.84$. The non-monotonic convergence displayed is typical of hybrid-mixed formulations. Good estimates are obtained for low execution times (full system, CG_IF solver), as shown in Table 8 for the 2×2 element mesh tests. The progressive p- and h-refinement of the Walsh solutions is illustrated in Fig. 16 for the estimates obtained for the σ_{xx} component of the stress field; the rows of the matrix represent improved p-refinements for a given finite element mesh and the columns represent improved h-refinements for Walsh approximations with the same degree.

The same problem is solved with the wavelet approximation ($N = 10$ and $m = 1$ for stresses and $m = 0$ for displacements). The values obtained are compared in Table 9 with the Walsh solutions, with degree $p = 5$, in terms of the estimates for the strain energy and the vertical displacement; T_PRE, T_SOL, T_POST and T_TOT denote the pre-processing, post-processing, solution and

Table 8. Estimates for the strain energy and the vertical displacement (elastic tests on the 2×2 element mesh with Walsh approximation).

Degree (p)	2	3	4	5	6
Dimension (N)	284	1,036	3,884	14,956	58,604
Time (sec.)	0.15	0.59	3.34	24.91	220.03
U/U_T	0.977	0.974	0.990	0.996	0.998
δ/δ_T (boundary)	0.950	0.967	0.988	0.996	0.998
δ/δ_T (domain)	0.958	0.971	0.990	0.997	0.999

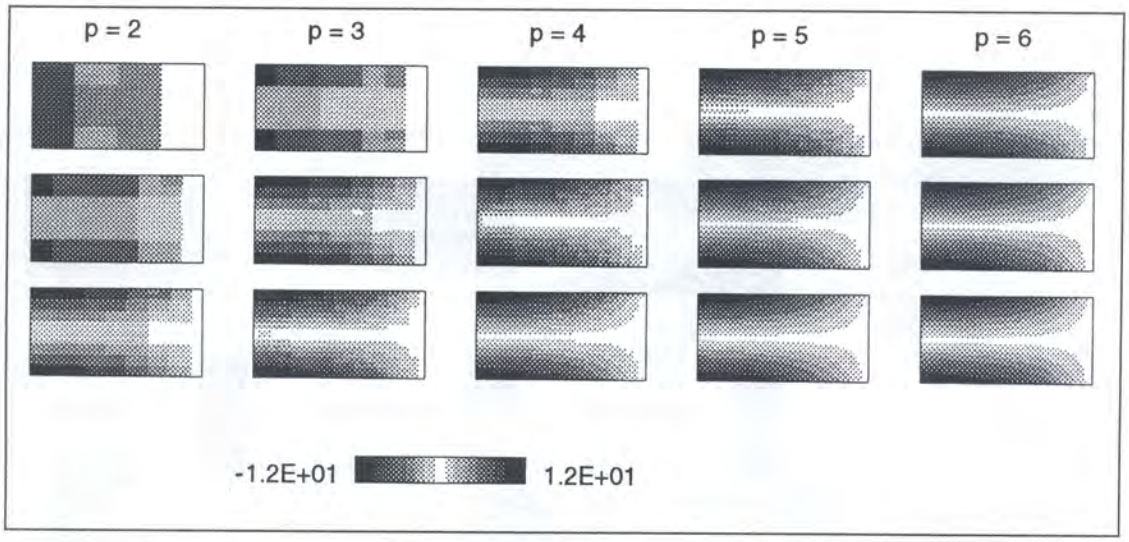

Fig. 16. Refinement of the σ_{xx} stress component in the simply supported beam.

Table 9. Comparation of the Walsh and wavelet solutions (elastic test, using the full system and the MA47 solver).

Mesh	Model	N	η	U/U_T	δ/δ_T	T_PRE	T_SOL	T_POST	T_TOT
1×1	Wavelet	419	53.75	0.999	1.001	3.23	4.07	0.82	8.12
	Walsh	3.770	99.73	0.989	0.990	0.06	4.80	0.48	5.34
2×2	Wavelet	1.644	87.81	0.999	1.001	3.31	58.07	1.44	62.82
	Walsh	14.956	99.93	0.996	0.996	0.21	24.65	2.41	27.27

total execution times, respectively, in seconds. The wavelet solution yields higher pre-processing times because the finite element matrices are computed through numerical integration, while the finite element matrices for the Walsh solutions are determined from general analytical expressions. Post-processing for the Walsh solution is performed as stated above. A grid of 128×128 points per element is used to represent the field approximations obtained with the wavelet model.

The results in Table 9 can be used to verify that the number of non-zero coefficients in the solving system is substantially larger for the wavelet model; the number of degrees of freedom it involves is substantially lower but it leads to a poorer sparsity index. Also, the structure of the system produced by the Walsh model is better exploited by the fill-in optimiser. Judging the relative performance using the parameters usually adopted to assess the accuracy of finite element models, strain energy and displacements, the information collected in Table 9 would suggest a clear

advantage for the Walsh solution. To block this effect, the solution times obtained by processing the condensed systems are shown in Table 10. Moreover, the graphic output of the stress field presented in Fig. 17 shows that the wavelet stress solutions are of better quality. It should be noticed that the static boundary conditions are satisfied by both approximations.

Table 10. Total execution time (in seconds) using the condensed system and MA47.

Mesh	Model	N	η	T_TOT
1×1	Wavelet	48	0.00	17.54
	Walsh	186	28.03	14.18
2×2	Wavelet	160	55.00	17.85
	Walsh	620	65.69	16.97

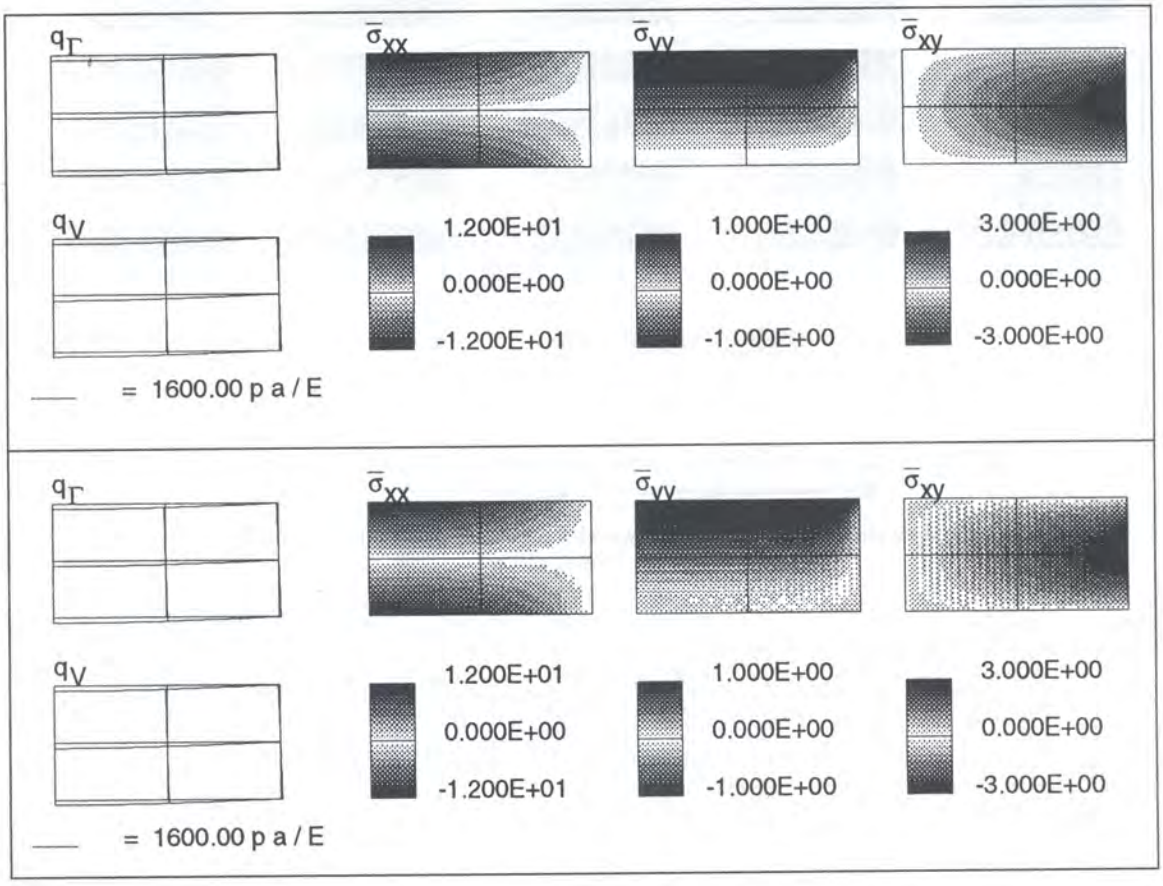

Fig. 17. Wavelet and Walsh displacement and stress estimates for the simply supported beam.

The wavelet approximation is used to obtain the elastoplastic response of the beam ($N = 10$ and $m = 1$ for stresses and $m = 0$ for displacements). The Mises-Hencky yield criterion is adopted. A 4×4 finite element mesh is adopted and in each element four critical cells are used to implement linear approximations of the plastic multiplier field. The solutions represented in Fig. 18 define three distinct stages in the elastoplastic response; the elastic limit stage, a stage during the development of the plastic hinge and the pre-collapse stage. They show that the approximation of plastic yielding should be improved, by refining the cells in the plastic zone and increasing the degree in the approximation of the plastic parameters to obtain a stronger enforcement of the yield condition.

The estimates obtained with the present approximation for the load parameter at the onset of yielding, $\lambda_E = 0.0894$, and at collapse, $\lambda_C = 0.130$, confirm the engineering beam theory results, defined by $\lambda_E = 0.083(3)$ and $\lambda_C = 0.125$, respectively.

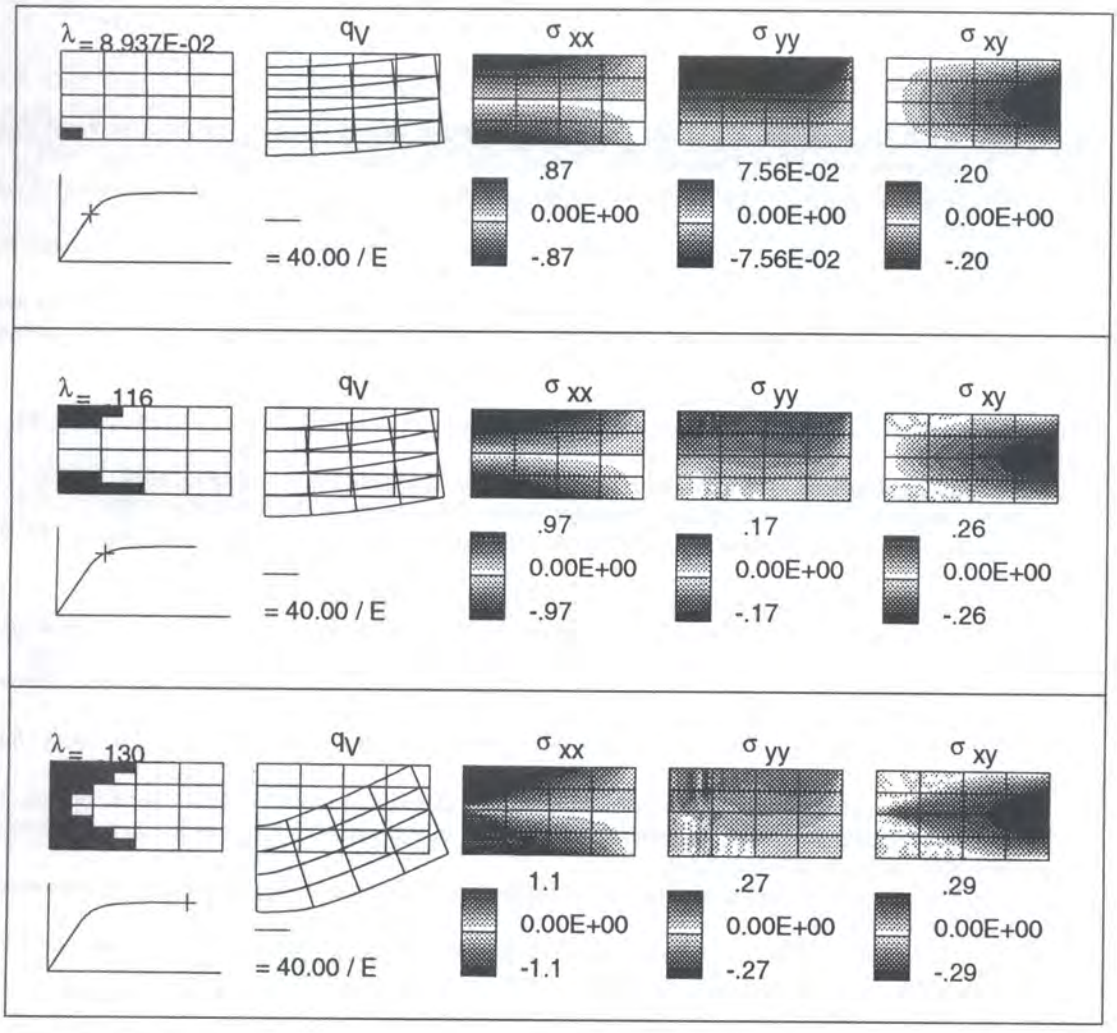

Fig. 18. Wavelet simulation of the elastoplastic response of the simply supported beam.

15. Closure

The results reported above justify a continued effort in the development of hybrid-mixed finite element formulations based on Walsh series and wavelet interpolation. The solutions obtained are computationally competitive and can provide accurate and stable estimates for the response of structures. Particular attention should be given to the following aspects. The formulation needs the support of a reliable and computationally competitive filter for spurious modes and should also be coupled with efficient p-adaptive procedures to exploit conveniently the hierarchical nature of the approximation functions. Improvements in the manipulation of these functions in a digital environment are certainly still possible, despite the substantial gains that have already been registered. Finally, better computational performances can still be achieved through the implementation of more sophisticated algorithms, adapted to the physics of the problems under analysis, and, naturally, by using parallel processing procedures, for which the hybrid-mixed formulations are unarguably well suited.

ACKNOWLEDGEMENT

This research has been sponsored by Junta Nacional de Investigação Cientìfica e Tecnológica (JNICT) as part of research project Praxis/2/2.1/CEG/33/94.

REFERENCES

[1] J.A.T. Freitas, J.P.B.M. Almeida, E.M.B.R. Pereira. Alternative hybrid formulations for the finite element method. In: J. Robinson, ed., *FEM Today and the Future*, 264–270, Antony Rowe Ltd., Wiltshire, 1993.

[2] J.A.T. Freitas, E.M.B.R. Pereira. Application of the Mathieu series to the boundary integral method. *Comput. & Struct.* **40**: 1307–1314, 1991.

[3] E.M.B.R. Pereira, J.A.T. Freitas. A mixed-hybrid finite element model based on orthogonal functions. *Int. J. Num. Meth. Engng.*, (to appear).

[4] L.M.S.S. Castro, J.A.T. Freitas. Hybrid-mixed finite element elastoplastic analysis based on Walsh and wavelet interpolation. In: M. Papadrakakis, ed., *Advanced Finite Element Solution* Techniques, CIMNE, Barcelona, (in press).

[5] J.L. Walsh. A closed set of orthogonal functions. *Ann. J. Math.*, **55**: 5–24, 1923.

[6] I. Daubechies. Orthonormal bases of compactly supported Wavelets. *Comm. on Pure & Appl. Math.*, **41**: 906–996, 1988.

[7] K.G. Beauchamp. *Applications of Walsh and related functions*, Academic Press, Orlando, 1984.

[8] R.S. Schalkoff. *Digital image processing and computer vision.* John Wiley & Sons, London, 1989.

[9] J.R. Williams, K. Amaratunga. Introduction to wavelets in engineering. *Int. J. Num. Meth. Engng.*, **37**: 2365–2388, 1994.

[10] G. Strang. Wavelets and dilation equations: a brief introduction. *SIAM Review*, **4**: 614–627, 1989.

[11] R. Glowinski, W.M. Lawton, L. Ravachol, E. Tenenbaum. Wavelet solution of linear and nonlinear elliptic, parabolic and hyperbolic problems in one space dimension. Aware, Inc., 1989, *SIAM* Philadelphia, 1990.

[12] J.A.T. Freitas, L.M.S.S. Castro. Digital interpolation in mixed finite element structural analysis. *Comput. & Struct.*, **44**: 743–751, 1992.

[13] J.A.T. Freitas. Duality and symmetry in mixed integral methods of elastostatics. *Int. J. Num. Meth. Engng.*, **28**: 1161–9, 1989.

[14] J.A.T. Freitas. Variational theorems in elastoplastic boundary element analysis. BEMXI, 65–79, Boston, 1989.

[15] J.A.T. Freitas, D.L. Smith. Existence, uniqueness and stability of elastoplastic solutions in the presence of large displacements. *SM Arch.*, **9**: 433–450, 1984.

[16] J.A.T. Freitas, D.L. Smith. Energy theorems for elastoplastic structures in a regime of large displacements. *J. MĆcanique*, **4**: 769–784, 1985.

[17] J.A.T. Freitas, D.L. Smith. Plastic straining, unstressing and branching in large displacement perturbation analysis. *Int. J. Num. Meth. Engng.*, **20**: 2077–2092, 1984.

[18] S. Pissanetzky. *Sparse matrix technology.* Academic Press, London, 1984.

[19] A. George, J.W.-H. Liu. *Computer solution of large sparse positive definite systems.* Prentice-Hall, Englewood Cliffs, 1981.

[20] L.M.S.S. Castro, J.A.T. Freitas. *Walsh function processing in the context of elastostatics.* Proc. EPMESCIV, 2: 1266–1273, The Dalian University of Technology Press, Dalian, 1992.

[21] L.M.S.S. Castro, J.A.T. Freitas. On the implementation of a mixed finite element formulation based on digital interpolation. Proc. Civil-Comp 93, 71–79, Edinburgh, 1993.

[22] L.M.S.S. Castro, J.A.T. Freitas. *Wavelets in mixed-hybrid finite element formulations.* Proc. EPMESCV, **2**: 1023–1028, Techno-Press, Seul, 1995.

[23] G.H. Golub, C. F Van Loan. *Matrix computations.* North Oxford Academic Publishers, London, 1986.

[24] E.A.W. Maunder, J.P.M. Almeida, A.C.A. Ramsay. A general formulation of equilibrium macro-elements with control of spurious kinematic modes — The exorcism of an old curse. *Int. J. Num. Meth. Engng.*, (in press), 1996.

[25] R.E. Paley. A remarkable set of orthogonal functions. *Proc. London Math. Soc.*, **34**: 241–279, 1932.

[26] K.W. Henderson. Comment on computation of the fast Walsh transform. *IEEE Trans. Comput.*, C-19, 850–851, 1970.

[27] G. Maier. Quadratic programming and the theory of elastic-perfectly plastic structures. *Meccanica*, **3**: 1–9, 1968.

[28] L. Corradi. A displacement formulation for the finite element elastic-plastic problem. *Meccanica*, **18**: 77–91, 1983.

[29] C. Comi, U. Perego. A unified approach for variationally consistent finite elements in elastoplasticity. *Comput. Meth. Appl. Mech. Engng.*, **121**: 323–344, 1995.

[30] J.A.T. Freitas, D.L. Smith. The post-collapse behaviour of rigid-plastic structures. *Eur. J. Mech. A/Solids*, **8**: 35–52, 1989.

[31] G. Maier, J. Munro. Mathematical programming applications to engineering plastic analysis. *AM Update*, 1982.
[32] G. Maier, D.L. Smith. Mathematical programming applications to engineering plastic analysis. *AM Update*, 1986.
[33] F.L. Alvarado. Manipulation and visualisation of sparse matrices. *ORSA J Computing*, **2**: 186–207, 1990.
[34] I.S. Duff, A.M. Erisman, J.K. Reid. *Direct methods for sparse matrices*. Oxford Press, Suffolk, 1986.
[35] J.A.T. Freitas, J.P.B.M. Almeida. A nonlinear projection method for constrained optimization. *Civil Engng. Syst.*, **1**: 294–300, 1984.
[36] I.S. Duff, J.K. Reid. The multifrontal solution of indefinite sparse symmetric linear equations. *ACM Trans. Math. Softw.*, **9**: 302–325, 1983.
[37] Harwell Subroutine Library. Advanced Computing Department. Harwell Laboratory, Oxfordshire, Release 11, 1993.
[38] J.P.B.M. Almeida. Janela: uma interface gráfica destinada à aplicaçã em problemas de Mecânica Computacional. *Rel. Int.*, IST, Lisbon, 1992.